

EG0700542

ESR Studies and Dating of Egyptian Gypsum at Ras Mala'ab, Sinai, Egypt

A.A. Abdel-Monem*, Y.A. Abdel-Razek*, G.M. Hassan**, H.M. Eissa**,
N.M. Rasheed*, and M. Morsy***.

* Nuclear Materials Authority, P. O. Box 530, El-Maadi, Cairo, Egypt., 11431.

** National Institute for Standards (NIS), P.O. Box 136, Giza, El-Giza, Egypt.

*** Department of Physics, Faculty of Science, Ain Shams University, Abbassia, Cairo, Egypt.,
11511.

ABSTRACT

A gypsum sample from the famous gypsum-anhydrite evaporitic deposit composing the Ras Mala'ab Formation, Upper Miocene, occurring at Ras Mala'ab, on the east coast of the Gulf of Suez, was subjected to (ESR) dosimetric studies. Also, (ESR) was used to date the formation or most recent recrystallization of that gypsum.

The gypsum derivative (ESR) spectrum is characterized by the large broad Fe^{2+} signal ($g=2.50$) and hf-sixtet Mn^{2+} signals. Only the characteristic gypsum signal ($G1$, $g=2.0040$) was detected between the third and fourth lines of the hf- Mn^{2+} which is attributed to the electron-center SO_3^- . This signal was sensitive to artificial γ -irradiation and showed significant enhancement using a γ -dose of 550 Gy. Also, the signal was very stable up to 400 °C.

The gypsum sample with a total dose (TD) of 1500 Gy, determined graphically by extrapolating the linear relationship between defect concentration and the artificial γ -doses for ($G1$, $g=2.0040$) and an annual dose (D) due to cosmic rays (0.3 mGy), yielded an age of 5.00 Ma. This could mean the age of formation or latest recrystallization of this gypsum deposit.

The geologic age assignment of the Ras Mala'ab Group including the evaporitic gypsum unit, is Middle to Late Miocene. It is directly overlain by the Pliocene clastics at the locality of Ras Mala'ab. This might suggest that these evaporitic gypsum facies represent the top of the Serravallian, (Mid-late) Miocene in the Gulf of Suez area. Since the Serravallian is between 14.8Ma and 11.2Ma ago, therefore, the ESR age of the Ras Mala'ab gypsum represents the latest recrystallization event of these gypsum deposits.

Key Words: Gypsum/ ESR dosimetry/ Dating/ Gulf of Suez.

INTRODUCTION

Gypsum ($\text{CaSO}_4 \cdot 2\text{H}_2\text{O}$) is a common evaporite mineral that has precipitated or crystallized from aqueous solution under dry or arid conditions. Gypsum has a monoclinic crystal structure containing four molecules in the unit cell.

Gypsum is found as extensive sedimentary deposits interbedded with limestones, red marls, green shales, sandstones, clay and rock salt. It is normally the first salt deposited in the evaporation of sea water, followed by anhydrite and halite as the salinity increases, which are followed, in rare cases, by the more soluble sulphates and other salts of Mg and K. Gypsum may also occur in many other ways:

as saline lake deposits, with native sulphur, around volcanic fumaroles, as an efflorescence on soils or in limestone caves, in the cap rock of salt domes and in the gossans over pyritic mineral deposits in limestone areas.

In Egypt, gypsum deposits are characteristic feature of the Miocene System. They are well developed especially in the central regions on both sides of the Gulf of Suez, where the Miocene succession is fully developed, where a complete and uniform sequence of deposition seem represented. At the Hammam Far'aon District where the studied gypsum sample was collected, the Miocene section starts with a flint-conglomerate bed followed by a marine series comprising (clay-grit-marl facies) marking marine transgression. Subsequently, the Miocene sea became shallower giving rise to series of lagoons where the Gypsum or Alabaster Series was laid down (~ 550m). This episode ended by another advance of the sea accompanied by the deposition of limestones and coral reefs with Nullipores, indicative of comparatively shallow sea. El-Gezeery and Mrzouk ⁽¹⁾ suggested the name Ras Mala'ab Group to the Miocene deposits in the Gulf of Suez region and assigned a middle to late Miocene age for the group. It is synonymous to the Evaporite Group of Said & El Heiny ⁽²⁾, mainly comprising evaporite facies. The gypsum facies contains some intercalations of clay, marl and sandstone as well as anhydrite, dolomites and limestones. The thickness of gypsum facies is 450m.

In this work, the ESR spectra of the natural gypsum before and after irradiation with γ -rays were studied. The physical properties of the identified ESR signals including their thermal stability and linear response to artificial irradiation are determined. The dosimetric characteristics are determined and evaluated. The calculated age will be discussed and correlated with the geological ages.

Gypsum ESR signals relevant to dating

Natural gypsum shows 4 types of ESR signals termed G1, G2, G3 and G4. These were detected in natural gypsum for ESR dating applications ⁽³⁾. The ESR signals are described briefly as follows:

G1 with isotropic ($g=2.004$) is identified as SO_3^- from the hf structure of ^{33}S (0.76 %, $I=3/2$, abundance 0.76%), and probably corresponds to B-center which has been assigned to a trapped electron at a vacancy or lattice defect ⁽⁴⁾.

G2 (CO_3^- or O_2^{3-}) is a hole-type center consisting of two magnetically non-equivalent sites enhanced by CO_3 impurity, ($g=2.008$) and ($g=2.006$).

G3 (CO_2^-) is an electron-type center attributed to (CO_2^-) and enhanced by K^+ , $g=2.001$ and $g_{\text{av}}=2.003$.

G4 (O_2H) $g=1.999-2.008$ ($A=0.2-0.5$). This signal corresponds to A-center, identified as O_2H ⁽⁴⁾.

In addition, marine gypsum may have the broad signal due to organic radicals at ($g=2.0045$) ⁽⁴⁻⁶⁾.

EXPERIMENTAL METHODS AND RESULTS

1. Materials and preparation

The gypsum sample was collected from the famous gypsum-anhydrite evaporitic deposit occurring at Ras Mala'ab quarry, Hammam Far'aon District, on the east coast of the Gulf of Suez about 20 km north of Abu Zeneima town. The gypsum produced is suitable for the cement industry and manufacture of the plaster of Paris.

The gypsum sample was ground and sieved to obtain the 200-300 μm size fractions. After being cleaned with acetone, aliquots of the sample were saved in a desiccator to dry gradually at room temperature. The aliquots prepared for irradiation and ESR measurements weighed 300 mg each.

2. ESR spectrometer operation and spectra

ESR spectra were measured with an ESR spectrometer (Bruker, EMX), in the X-band at room temperature using a standard rectangular cavity. The ESR spectrometer operating parameters were chosen to provide the maximum signal-to-noise ratio for non-distorted signal as follows: Microwave frequency 9.7 GHz with 100 kHz field modulation, magnetic field modulation amplitude 1 gauss (G) with field-sweeping rate of 100 G/164s and response time constant 40 ms. The Lande' g-factor and intensity of the ESR signal were calibrated using standard MgO doped with Mn^{2+} and weak pitch doped with (13% KCl) respectively. The microwave power was optimized for the ESR signal ($g=2.0040$) and the maximum intensity value was found at microwave power of 6.331 mW for the gypsum samples, (Fig. 1).

Natural gypsum from Ras-Malaab, Sinai, Egypt, was investigated by ESR spectrometer. The derivative ESR spectrum of gypsum at room temperature is shown in (Fig. 2). The spectrum is characterized by the prominent Fe^{2+} and hf sextet Mn^{2+} signals. The characteristic ESR isotropic signal of natural gypsum (G1) at $g=2.0040$ is illustrated in (Fig. 3)⁽³⁾. This detected characteristic signal will be investigated to evaluate its applicability to ESR dosimetric work as well as dating techniques.

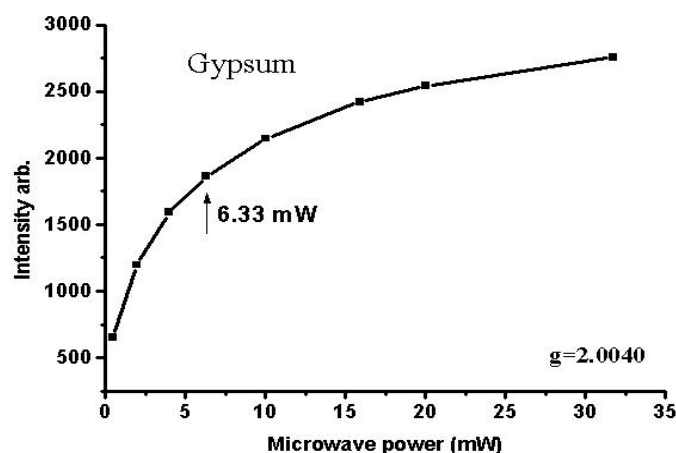


Fig. 1: Variation of ESR intensity with microwave power for natural gypsum at $g=2.0040$.

Intense ESR signals (G1 and G2) associated with defects in gypsum were observed during ESR dating of gypsum^(7,8). The dating signal (G2) at ($g=2.008$) and also (G3) were not observed presumably due to the absence of CO_3^{2-} impurity in gypsum.

3. Determination of the total accumulated dose (TD)

The ESR signal ($g=2.0040$) used for dating natural gypsum exhibited positive response to γ -irradiation using a dose of 550 Gy as shown in (Fig. 4).

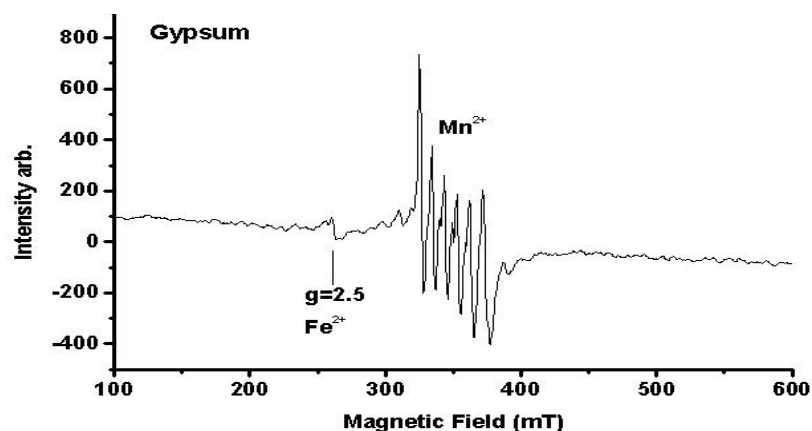


Fig. 2: ESR derivative spectrum of natural gypsum from Sinai at room temperature.

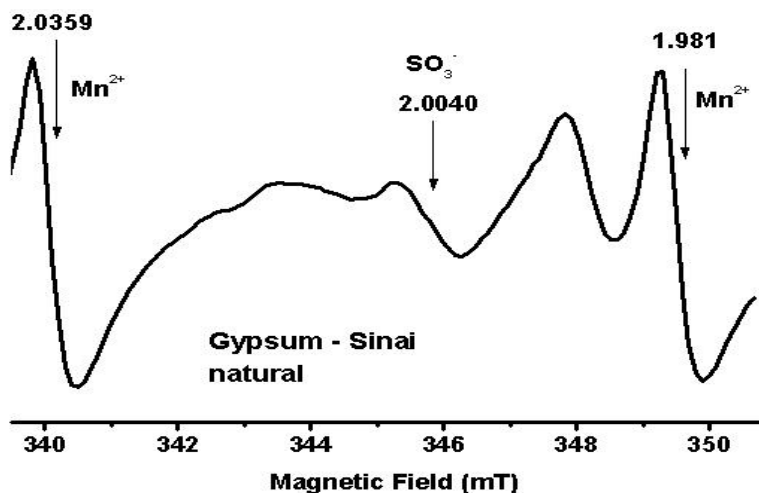


Fig. 3: Characteristic ESR signal at $g=2.0040$ as appeared in the ESR spectrum of natural gypsum at room temperature between the third and the fourth lines of hf-sixtet Mn^{2+} .

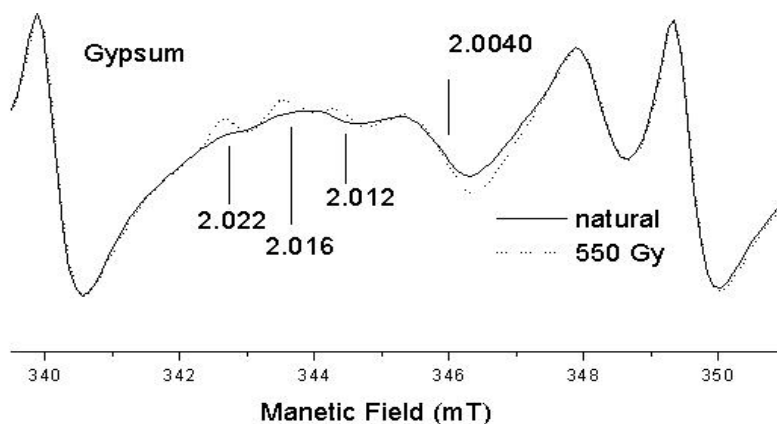


Fig. 4: Enhancement of the ESR signal at $g=2.0040$ for Sinai gypsum by γ -irradiation.

Figure (5) shows the growth of the intensity of the ESR characteristic signal at $g=2.0040$ with the irradiating γ -doses up to 26kGy. The saturation dose of the mineral is also shown on the figure. The equation ⁽⁹⁾

$$I(Q) = I_s (1 - e^{-(Q+TD)/SD}) \quad (1)$$

where

I_s = Saturation intensity at the ESR characteristic signal; SD = Saturation dose; was used to obtain the total dose (TD) by adjusting the quantities I_s , SD and TD until the calculated line (dotted line in Fig. 5) passes through a maximum number of experimental points (solid line). The dotted line intersected the γ -dose axis at a dose of 1.5kGy which is the estimated (TD) for the investigated gypsum.

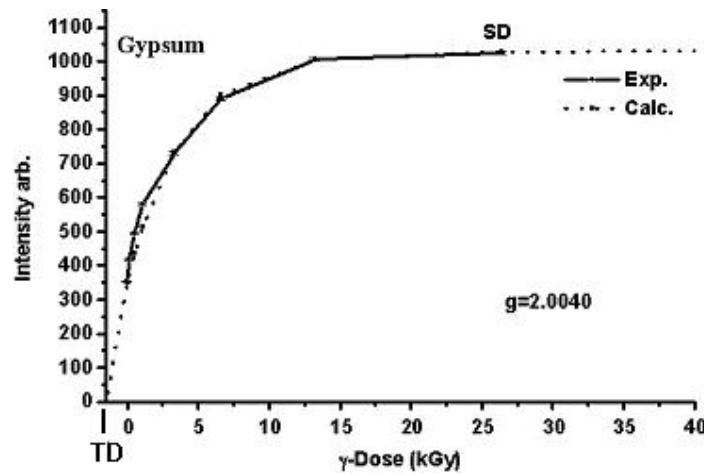


Fig 5: Total dose (TD) and saturation dose (SD) of gypsum for ESR signal at $g=2.0040$.

4. Determination of the saturation lifetime (τ_s)

The saturation lifetime (τ_s) is obtained by dividing the saturation dose (SD), (Fig. 5), by the annual dose due to the cosmic rays (0.3 mGy/a) ⁽⁹⁾. This yields a value of 68.7 Ma.

5. Determination of defects lifetime (τ)

Isochronal annealing technique was used to determine the lifetime of defects (τ) in the gypsum samples after γ -irradiation at 26 kGy. The γ -irradiated samples were step-heated from $100-400^\circ\text{C}$, each step was an increment of 25°C with an annealing time of 15min at each step. After each annealing step, samples were left to cool to room temperature and the ESR signal intensities at ($g=2.0040$) were measured. The effects of the isochronal heating on the ESR signal intensity in the studied samples are shown in (Fig. 6). The lifetimes (τ) of the ESR signal was determined using the equation ⁽⁹⁾:

$$\log_{10} \tau = (16.409/T)T_{a10} - 12.477, \quad (2)$$

where

T = The geothermal temperature in degrees Kelvin ($^\circ\text{K}$).

T_{a10} = The annealing temperature at which the ESR signal intensity is 90% of its intensity at the previous annealing temperature step ($^\circ\text{K}$).

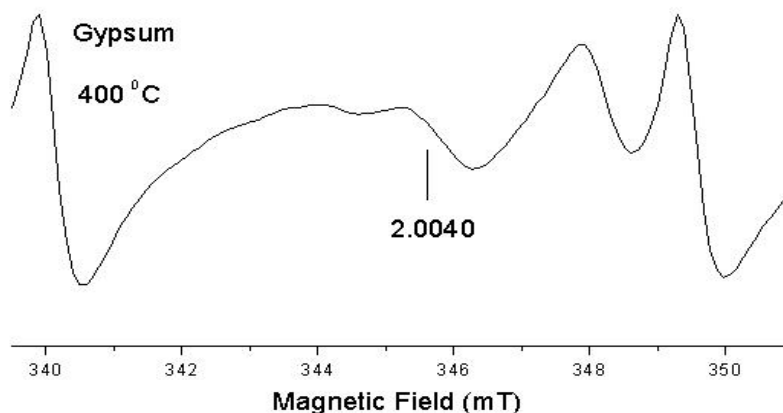


Fig. 6: Stability of the ESR signal at $g=2.0040$ for gypsum from Sinai against temperature

The (T_{a10}) were determined from the isochronal annealing curve (Fig. 7). The geothermal temperature (T) is estimated at 25°C as an average annual atmospheric temperature for the desert conditions where the sample was collected. The calculated defect lifetime (τ) for gypsum was 28 Ma; using the above equation.

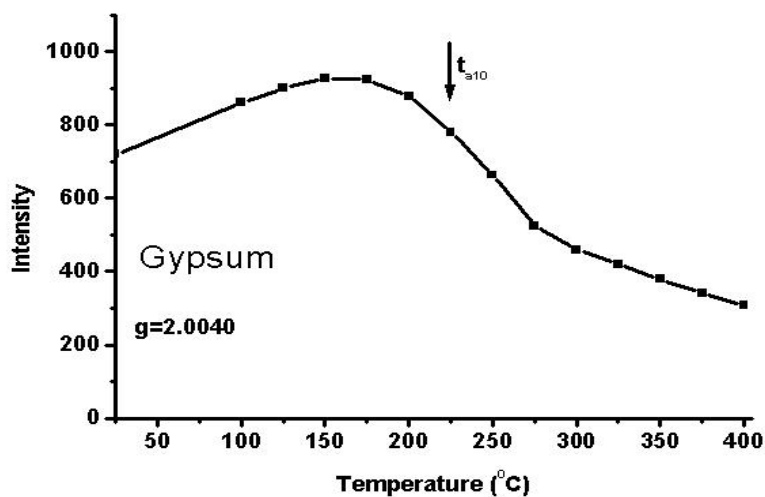


Fig. 7: Isochronal annealing curve of gypsum at temperatures from 100 to 400°C .

6. Determination of the effective lifetime (τ_e)

The effective lifetime (τ_e) for the gypsum sample was determined according to the equation⁽⁹⁾:

$$1/\tau_e = 1/\tau + 1/\tau_s, \quad (3)$$

which yielded a value of 21.2 Ma.

7. ESR age

The age of the gypsum sample was obtained by deviding the total dose (TD) by the natural annual dose (from cosmic rays). This yields an age of 5.00 Ma.

DISCUSSION AND CONCLUSION

Gypsum is useful for ESR dating and has been widely applied to a number of different geological materials and problems requiring determining the chronology. These applications of ESR dating of gypsum precipitated in dry caves and volcanic caves ⁽¹⁰⁾; gypsum precipitated in playa lakes as lacustrine terraces at paleolithic sites ⁽⁸⁾; gypsum crystal precipitated at fault surfaces after displacement ⁽⁵⁾, and gypcrete which is a gypsum cemented crust formed in arid climates in some playa-lake bed-rock environment ^(11,12). The main application of ESR dating of gypsum was for the marine stratigraphic gypsum, where marine gypsum crystals of sea origin are dated using G1 signal at $g=2.0040$. Consistent results with stratigraphy have been reported ^(5,6,13-15). However, the possibility of an overlapping organic signal at $g=2.0045$ must be considered. The contribution of such a broad signal if present in the spectrum should be subtracted for a precise age determination, ⁽⁶⁾.

The ESR age of the gypsum sample from Ras Malaab area is 5.00 Ma. The geologic age assignment of the Ras Malaab Formation dominated by evaporitic gypsum is middle to late Miocene. This is based on the fact that it overlies the Kareem Formation of the Gharandal Group and it underlies directly the Pliocene clastics. This designated Ras Mala'ab Group⁽¹⁾ is synonymous with the Evaporitic Group⁽²⁾. However, more recent work^(16,17), considered the evaporite facies to have deposited during the Serravallian (Mid-late Miocene). Ouda and Masoud⁽¹⁷⁾, identified three cycles each one comprising an early evaporite phase followed by an open marine one during the Serravallian. The third and top-most cycle (Feiran-Hammam Far'aon Cycle) includes the Ras Mala'ab evaporitic deposits, i.e., representing the top of the Serravallian. Therefore, the gypsum facies could be considered to represent the top of the Miocene in the Gulf of Suez area. According to the Geologic Time Scale of the Phanerozoic Eon, the boundary between the Miocene and Pliocene is put at 5.00-5.50 Ma ago ⁽¹⁸⁾. However, Grandstein and Ogg⁽¹⁹⁾, put the age of the Serravallian (Mid-late Miocene) between 14.8Ma and 11.2Ma. In this case, the ESR age of the gypsum at Ras Malaab obtained at 5.00 Ma using the ESR signal at ($g=2.0040$) represents the latest recrystallization event of these gypsum deposits.

REFERENCES

- (1) M.N. El-Gezeery and I.M. Marzouk, (eds.); The Stratigraphic Sub-Committee of the National Committee of Geological Sciences (NCGS): Miocene rock stratigraphy of Egypt. *J. Geol.*, 18, 1 (1974).
- (2) R. Said and I. El Heiny; Planktonic foraminifera from the Miocene rocks of the Gulf of Suez region. *Contr. Cushman Found. Foram. Res.*, 18, 14 (1967).
- (3) M.Kasuya, S. Brumby and J.Chappel; ESR signals in gypsum single crystals: implications for ESR dating. *Nucl. Tracks*, 18, 329 (1991).
- (4) A.R.P.L. Albuquerque and S. Isotani; The EPR spectra of x-ray irradiated gypsum. *J. Phys. Soc. Japan*, 51, 1111 (1982).
- (5) S. Ikeda and M.Ikeya; ESR signals in natural and synthetic gypsum: An application of ESR to the age estimation of gypsum precipitates from San Andreas Fault. *Jpn. J. Appl. Phys.*, 31, L136 (1992).
- (6) K.S.V.Nambi; : ESR and TL dating studies on some marine gypsum crystals. *PACT*, 6, 314 (1982).
- (7) M. Ikeya; ESR as a method of dating. *Archaeology*, 2, 147 (1978).
- (8) M. Ikeya (Ed.); EPR Dating and Dosimetry. Ionics, Japan, 538p (1985).
- (9) M.Ikeya; New Applications of Electron Spin Resonance: Dating, Dosimetry and Microscopy. World Scientific Publ. Co., Singapore, 500p (1993).
- (10) B. W. Moore and B. G.Nicholas; *Speleology: The Study of Caves* (Health & Company, Mass.) (1964).

- (11) Y.Chen, J. Lu, A. V. Arakel and G. Jackson; ^{14}C and ESR dating of calcrete and gypcrete cores from the Amadeus Basin, Northern Territory, Australia. *Quatern. Sci. Rev.* 7. 447 (1988).
- (12) Y. Chen, A. V. Arakel and J. Lu; Investigation of sensitive signals due to γ -rays irradiation of chemical precipitates. A feasibility study for ESR dating of gypsum, phosphate and calcrete deposits. *Appl. Radiat. Isot.*, 40 (10/12). 1163 (1989).
- (13) S. Ikeda, M. Ikeya and N. Kashima; ESR dating of gypsum speleothems. *J. Speleol. Soc. Jpn.* 14. 68 (1989).
- (14) T. Omura and M. Ikeya; *Geochem J.* 29. 317 (1995).
- (15) U. Ulusoy; ESR studies of Anatolian gypsum. *Spectrochimica Acta Part A*, 60. 1359 (2004).
- (16) B. Burser and E. Philobos; The sedimentary expression of rifting in the NW Red Sea, Egypt. *Geol. Soc. Egypt, Sepc. Publ.* 1. 1 (1993).
- (17) K.H. Ouda and M. Masoud; Sedimentation history and geological evolution of the Gulf of Suez during the late Oligocene-Miocene. *Geol. Soc. Egypt, Sepc. Publ.* 1. 47 (1993).
- (18) G.S.Odin, D.Carvy, N.M. Gale, and W.I.Kennedy; The Phanerozoic time scale in 1981. In: G.S. Odin (ed.). *Numerical Dating in Stratigraphy*, vol. 2, 957-960. John Wiley, New York (1982).
- (19) F. Grandstein and J. Ogg; A Phanerozoic Time-Scale. *Episodes*, 19 (1&2) (1996).